Ailanthus altissima mapping from multi-temporal very high resolution satellite images

Tarantino, Cristina; Casella, Francesca; Adamo, Maria; Lucas, Richard; Beierkuhnlein, Carl; Blonda, Palma

Published in:
ISPRS Journal of Photogrammetry and Remote Sensing

DOI:
10.1016/j.isprsjprs.2018.11.013

Publication date:
2019

Citation for published version (APA):
Tarantino, C., Casella, F., Adamo, M., Lucas, R., Beierkuhnlein, C., & Blonda, P. (2019). *Ailanthus altissima* mapping from multi-temporal very high resolution satellite images. *ISPRS Journal of Photogrammetry and Remote Sensing*, *147*, 90-103. https://doi.org/10.1016/j.isprsjprs.2018.11.013

ISPRS Journal of Photogrammetry and Remote Sensing 147 (2019) 90–103

Contents lists available at ScienceDirect

ISPRS Journal of Photogrammetry and Remote Sensing

journal homepage: www.elsevier.com/locate/isprsjprs

Ailanthus altissima mapping from multi-temporal very high resolution satellite images

Cristina Tarantino[a,*], Francesca Casella[b], Maria Adamo[a], Richard Lucas[c], Carl Beierkuhnlein[d,e,f], Palma Blonda[a]

[a] Institute of Atmospheric Pollution Research (IIA), National Research Council (CNR), c/o Interateneo Physics Department, Via Amendola 173, 70126 Bari, Italy
[b] Institute of Sciences of Food Production (ISPA), National Research Council (CNR), Via Amendola 122/D-O, 70126 Bari, Italy
[c] Institute of Geography and Earth Sciences, Aberystwyth University, Aberystwyth, Ceredigion SY23 2EJ, United Kingdom
[d] Chair of Biogeography, University of Bayreuth, 95440 Bayreuth, Germany
[e] Bayreuth Center of Ecology and Environmental Research, BayCEER, 95440 Bayreuth, Germany
[f] Geographical Institute Bayreuth, GIB, 95440 Bayreuth, Germany

ARTICLE INFO

Keywords:
Invasive species
Alien species
Ailanthus altissima mapping
multi-temporal WorldView-2 data
Remote sensing
Novel ecosystems

ABSTRACT

This study presents the results of multi-seasonal WorldView-2 (WV-2) satellite images classification for the mapping of *Ailanthus altissima (A. altissima),* an invasive plant species thriving in a protected grassland area of Southern Italy. The technique used relied on a two-stage hybrid classification process: the first stage applied a knowledge-driven learning scheme to provide a land cover map (LC), including deciduous vegetation and other classes, without the need of reference training data; the second stage exploited a data-driven classification to: (i) discriminate pixels of the invasive species found within the deciduous vegetation layer of the LC map; (ii) determine the most favourable seasons for such recognition. In the second stage, when a traditional Maximum Likelihood classifier was used, the results obtained with multi-temporal July and October WV-2 images, showed an output Overall Accuracy (OA) value of ≈91%. To increase such a value, first a low-pass median filtering was used with a resulting OA of 99.2%, then, a Support Vector Machine classifier was applied obtaining the best *A. altissima* User's Accuracy (UA) and OA values of 82.47% and 97.96%, respectively, without any filtering. When instead of the full multi-spectral bands set some spectral vegetation indices computed from the same months were used the UA and OA values decreased. The findings reported suggest that multi-temporal, very high resolution satellite imagery can be effective for *A. altissima* mapping, especially when airborne hyperspectral data are unavailable. Since training data are required only in the second stage to discriminate *A. altissima* from other deciduous plants, the use of the first stage LC mapping as pre-filter can render the hybrid technique proposed cost and time effective. Multi-temporal VHR data and the hybrid system suggested may offer new opportunities for invasive plant monitoring and follow up of management decision.

1. Introduction

Alien plants, also termed non-native, exotic or allochthon plants, can modify diversity and functioning of ecosystems especially when they exhibit invasive tendencies (Pyšek and Richardson, 2010; Foxcroft et al., 2013). At present, highly competitive woody invasive species, such as *A. altissima (Mill.) Swingle,* are causing impoverishment in natural habitats and consequent economic losses (Kowarik and Saumel, 2007; Bostan et al., 2014; Niphadkar et al., 2017).

To address problems caused by invasive alien species, reduce and monitor their negative impact on the environment, the European Member States have approved a specific regulation (Regulation 1143/2014). This act supports interventions aimed at prevention, early detection, rapid eradication and management of invasive species spreading.

Traditionally, early detection of alien species has been based on evidence from in-field inspections. The resulting maps can be very detailed and rich not only in information on the distribution of specimen, but also on possible management options as eradication and monitoring. Although useful, in-field data and provisions can be burdened by limits. These include aspects such as workload, area accessibility, extent and speed of alien plants invasion. Due to these factors, extensive

* Corresponding author.
E-mail addresses: cristina.tarantino@iia.cnr.it (C. Tarantino), francesca.casella@ispa.cnr.it (F. Casella), adamo@iia.cnr.it (M. Adamo), rml@aber.ac.uk (R. Lucas), carl.beierkuhnlein@uni-bayreuth.de (C. Beierkuhnlein), palma.blonda@iia.cnr.it (P. Blonda).

https://doi.org/10.1016/j.isprsjprs.2018.11.013
Received 1 June 2018; Received in revised form 12 November 2018; Accepted 12 November 2018

Table 1
Studies on invasive species grouped by HS and MS, sorted by spatial resolution. Legend: Hyperspectral (HS); Multispectral (MS); Multiple Endmember Spectral Mixture Analysis (MESMA); Spectral Angle mapper (SAM); Maximum Likelihood (ML); Mixture Tuned Matched Filtering (MTMF); Support Vector Machine (SVM); Random Forest (RF).

Authors	Year	Species	Data sources	Country	Method of classification	Temporal analysis	N. classes	Accuracy%	
Somers et al.	(2013a), (2013b)	*Morella, Metrosideros*	HS, Hyperion (30 m)	Hawai	Supervised by data (MESMA)	**Multi-temporal**	3	90.0	OA
Pengra et al.	2007	*Phragmites australis*	HS, Hyperion (30 m)	USA	Supervised by data (SAM)	Mono-temporal	2	81.4	
Mirik et al.	2013	*Carduus nutans*	HS, Aisa (4 m)		Supervised by data (SVM)		2	91.0	
Ustin et al.	2002	*Carpobrotus edulis and jubata, Foeniculum vulgare, Arundo donax*	HS, Aviris (4 m)		Supervised by data (SAM, K-Means, ML)		4	> 82.0	
Glenn et al.	2005	*Euphorbia esula*	HS, HyMap (3 m)		Supervised by data (MTMF)		2	93.0	
Andrew and Ustin	2008	*Lepidium latifolium*	HS, HyMap (3 m)		Supervised by data (MTMF)		2	90.0	
Atkinson et al.	2014	*Solanum mauritianum*	HS, Eagle (2.4 m)	South Africa	Supervised by data (SVM)		2	91.0	
Groβe-Stoltenbeg et al.	2018	*Acacia longifolia*	HS, Eagle/Hawk (2 m) and LIDAR	Portugal	Supervised by data (RF)		2	81.0	UA
Da Luz and Crowley	2010	***Ailanthus altissima***	HS, Thermic, Sebass (1 m)	USA	Supervised by data (MTMF)		50	ranking matrix	
De Sa' et al.	2017	*Acacia longifolia*	MS, Landsat TM/ETM + (30 m)	Portugal	Supervised ML and rule-based	Mono-temporal	19	78.5	UA
Ng et al.	2017	*Prosopis and Vachellia*	MS, Sentinel-2 (20 m)	Kenya	Supervised by data (RF)		4	91.0	OA
Gavier-Pizarro et al.	2012	*Ligustrum lucidum*	MS, Landsat ETM + (30 m)	Argentina	Supervised by data (SVM)	**Multi-temporal**	3	84.0	
Niphadkar et al.	2017	*Lantana camara*	MS, WorldView-2 (2 m.)	India	Supervised by data (ML) and Supervised by rules (object based)		9	60.0	
Everitt et al.	2005	*Arundo donax*	MS, Quickbird (2.8 m)	USA	Unsupervised (Isodata)	Mono-temporal	5	83.0	
Monteiro et al.	2017	*Acacia dealbata*	MS, WorldView-2 (2 m)	Portugal	Supervised by data (RF)		2	91.3	
Peerbhay et al.	2016	*Solanum mauritianum*	MS, WorldView-2 (2 m)	South America	Unsupervised RF		3	91.3	
Müllerova et al.	2017a	*Fallopia japonica*	MS, Pleiades (2 m) UAV (drone; 5 cm)	Czech Republic	Supervised by data (SVM-RF, July) Supervised by data (SVM, August)		2	85.0 78.0	
	2017b	*Robinia pseudoacacia*	MS, WorldView-2 (2 m) UAV (drone; 5 cm)		Supervised by data (ML)		2	81.0 81.0	UA
Dvorak et al.	2015	***Ailanthus altissima***	MS, UAV (drone; 6 cm)		Hybrid: supervised by rules and data		4	/	

in-field inspections can be both time consuming and costly especially in areas where implementation of monitoring would require feasibility and quick management decisions (Sitzia et al., 2016).

Remote Sensing (RS) data and techniques can not only allow coverage of large areas repetitively, but also provide data for areas difficult or dangerous to reach, such as the tiger reserve described in (Niphadkar et al., 2017). Thus, they represent an efficient add-on or even an alternative to in-field inspections (Nagendra et al., 2013; Peerbhay et al., 2016).

RS data have already been used in alien plant detection. An interesting review on the subject is provided by Bradley (2014). In Table 1, we provide an overview of the most recent applications along with the classification methods, the specific satellite and/or airborne data, namely hyperspectral or multispectral, and the results obtained, i.e. Overall Accuracy (OA) or User's Accuracy (UA), for each invasive species investigated. Most of the papers listed in this Table adopted and evaluated different supervised techniques, however, in the last column, only the best result of each study is reported for comparative reasons. The supervised classifiers employed by the different authors include the well-known Maximum Likelihood (ML) (Ustin et al., 2002; Niphadkar et al., 2017; De Sa' et al., 2017; Müllerova et al., 2017a; 2017b), the Support Vector Machine (SVM) (Gavier-Pizarro et al., 2012; Mirik et al., 2013; Atkinson et al., 2014), the Random Forests (RF) (Monteiro et al., 2017; Ng et al., 2017; Groβe-Stoltenbeg et al., 2018), the Mixture Tuned Matched Filter (MTMF) (Glenn et al., 2005; Andrew and Ustin, 2008; Da Luz and Crowley, 2010) and the Spectral Angle Mapper (SAM) (Ustin et al., 2002; Pengra et al., 2007).

Even though *A. altissima* has been recognized as one of the most wide spread and harmful invasive plants in both the USA (Burkholder et al., 2011) and Europe (www.europe-aliens.org), only two of the papers reported in Table 1 have focussed on the mapping of this species (Da Luz and Crowley, 2010; Dvorak et al., 2015) using either hyperspectral (HS) aerial or multi-spectral (MS) UAV data.

In the Mediterranean basin *A. altissima* is spreading rapidly due to both the dramatic climatic change taking place in this region and the consequent land abandonment (Bardsley and Edwards-Jones, 2007). Reportedly, this species can invade fallow land and endanger ecosystems more rapidly than any of the native species (Walker et al., 2017). Therefore, the detection of this plant would require more extensive remote sensing studies.

In light of this need, the present study has two main objectives: the first aims at verifying the effectiveness of multi-spectral and multi-temporal Very High Resolution (VHR) satellite data (i.e., WV-2) in the mapping of *A. altissima* in the Mediterranean area. The second objective is to verify the effectiveness of a two-stage hybrid classification scheme in the plant investigation approach. The first classification stage uses a knowledge-driven learning procedure, which can provide a multiple class Land Cover (LC) map without requiring in-field reference data (Adamo et al., 2015; Lucas at al., 2015). The deciduous layer extracted from this LC map will be used as a pre-filter for the input data to the second classification stage. The latter is a supervised data-driven classifier which can discriminate two classes (i.e., *A. altissima* and other deciduous) by analysing only the pixels belonging to the deciduous vegetation layer of the LC map obtained in the first stage.

The two-stage approach proposed is novel and useful since it can reduce not only classification complexity, but also time and costs involved by in-situ reference data collection.

The study area is located in the "Murgia Alta", a protected site in Southern Italy which belongs to the European Natura 2000 network, i.e., a coordinated network of core breeding and resting sites for rare and threatened species, and some rare natural habitat types which are protected (http://ec.europa.eu/environment/nature/natura2000/index_en.htm).

Besides providing a comprehensive contribution to an early-on and cost-effective detection and management of the globally important invader *A. altissima*, the present study will try to determine the best season (s) to carry out identification and mapping in the "Murgia Alta".

2. Materials and methods

2.1. Alien species studied

Ailanthus altissima, also known as tree-of-haven or Chinese sumac, is an invasive deciduous plant of Asian origin belonging to the Simaroubaceae family. The invasive plant can yield up to more than 1 Mio seeds annually in adulthood (Wickert et al., 2017). The tree is endowed with an exceptionally wide window of seed production which can last over 100 years. The invasive capacity of *A. altissima* includes its ability to reproduce equally well both by seed and asexually (Kowarik, 1995; Richardson et al., 2000). The plant winged seeds can be dispersed by wind, water and machinery, while its vigorous root system can generate numerous suckers and progeny plants (Planchuelo et al., 2016).

Ailanthus altissima saplings grow very quickly with considerable vigor, reaching meters of height in a short time. Moreover, the species can adapt to different type of soil and water regime (Kowarik & Saumel, 2007), thus, it can easily reach almost any area and cause severe ecological damage (Casella & Vurro, 2013). At present, *A. altissima* is reported as one of the most important causes of local and regional biodiversity loss (Chornesky & Randall, 2003). The alien plant can cause ecosystem degradation, diminishing both abundance and survival of native species (Casella et al., 2015a, 2016).

As a consequence, *A. altissima* is considered to be a threatening invasive alien species in both Europe (www.europe-aliens.org) and North America (Burkholder et al., 2011). In Italy, the species has spread through all the southern regions (Celesti-Grapow et al., 2010).

2.2. Site description

The study area covers 500 km^2 located in the "Murgia Alta" Natura 2000 protected area, within the Apulia region, Southern Italy (Fig. 1a). The altitude of the area is around 700 m above the sea level and its climate is typically the one of the sub-Mediterranean basin (Mairota et al., 2013).

According to the list of habitats reported in Annex 1 (Appendix A) attached to the European Habitat Directive (Council Directive 92/43/EEC), the most important habitat types in this area include *semi-natural and natural dry grasslands and scrubland facies on calcareous substrates,* important orchid sites coded as 6210* and 6220 and *pseudo-steppe with grasses and annuals* (the symbol * indicates priority habitat types in Annex I to the European Habitat Directive; specifically, 6210* is an endemic habitat in Murgia Alta). The "Murgia Alta" represents one of the most important areas for the conservation of these types of ecosystems in Europe and it is also considered a haven for the conservation of birds, wildlife and priority species (Birds Directive, Council Directive 2009/147/EEC).

These unique ecosystems are under pressure and in danger of destruction due to agricultural intensification, urbanization, arson and land abandonment. Climatic changes and *A. altissima* invasion are also contributing to further degradation and pressure in the area (Mairota et al., 2013, 2015). In the Murgia Alta area the invader can grow mainly: (a) in semi-natural and natural grasslands fields due to shepherds practices abandonment; (b) at the edges of cultivated fields, mainly herbaceous areas. Within such fields, the invader is generally controlled by the farmers through regular ploughing or other agricultural practices.

Occasional fires occurring in this area can also be favoured by the proliferation of this plant (Crandall & Knight, 2018).

2.3. Data availability

Ailanthus altissima mapping was carried out by means of four, cloud-

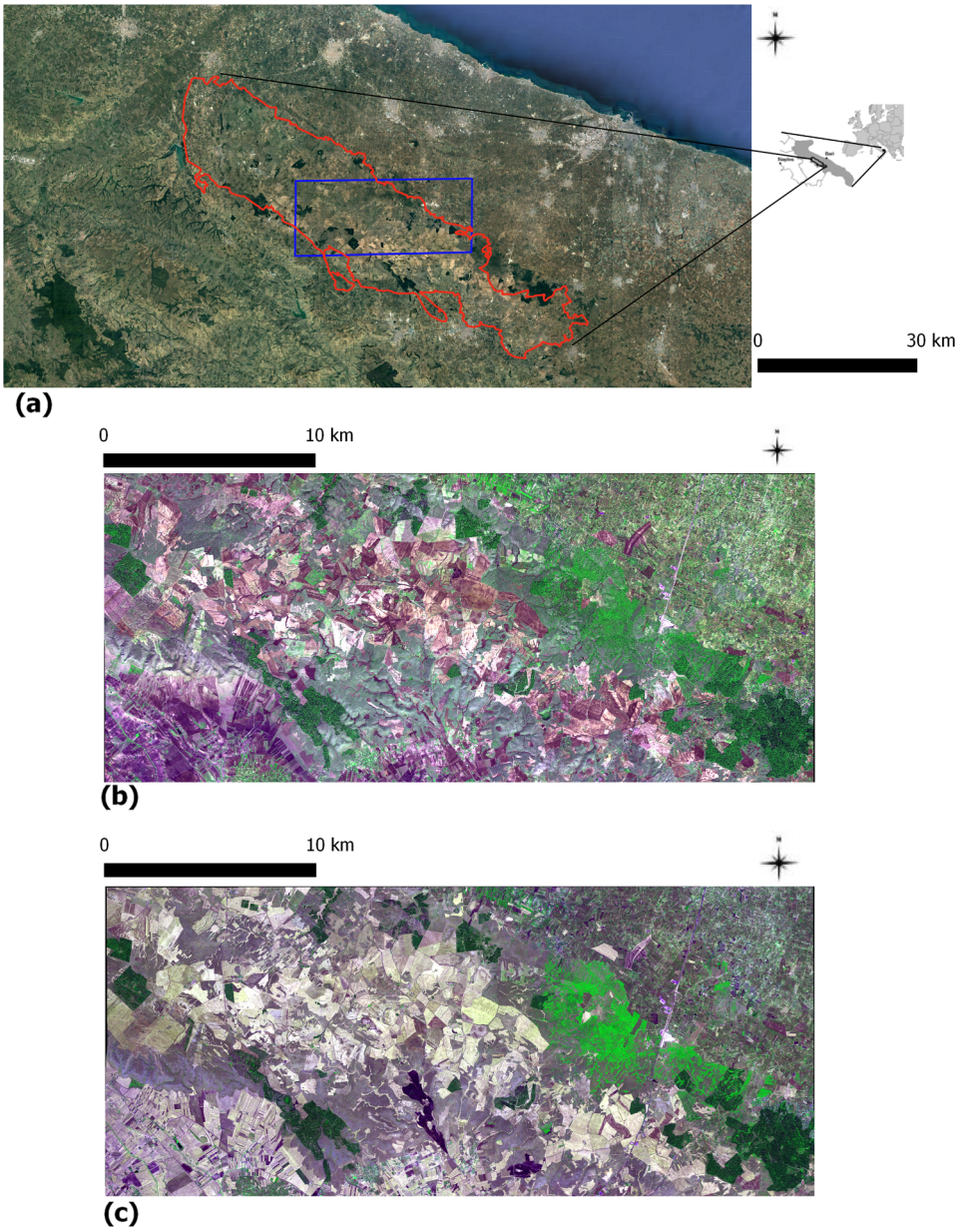

Fig. 1. "Murgia Alta" Natura 2000 site. (a) Location and extension of "Murgia Alta" protected area in red line. The 500 km^2 analyzed area in blue line. (b) WV-2 input image, 2 m resolution, October 5th, 2011. (c) WV-2 input image, 2 m resolution July 6th, 2012. False Colour Composite: Band 5, Band 7, Band 2.

free, multi-seasonal WV-2 images. WV-2 is a VHR satellite that can acquire data within the 0.4–1.40 μm spectral range of eight bands having spatial resolution of two meters and swath width of 16.4 km. The eight spectral bands of WV-2 include four standard bands situated in the BLUE (0.450–0.510 μm), GREEN (0.510–0.580 μm), RED (0.630–0.690 μm) and NIR1 (0.770–0.895 μm) and additional four bands which are COASTAL (0.400–0.450 μm), YELLOW (0.585–0.625 μm), RED EDGE (0.705–0.745 μm) and NIR-2 (0.860–1.400 μm).

In the present study, all the WV-2 spectral bands of the multi-temporal data set were considered following the techniques adopted by Omer et al. (2015). In their investigation of endangered tree species, Omer et al. (2015) reported that, by using the full set of WV-2 spectral bands, they obtained better results than when using only 4 bands, either standard or additional bands.

The images analysed were provided by the European Space Agency (ESA) under the Data Warehouse 2011–2014 policy within the FP7-SPACE BIO_SOS project (www.biosos.eu). They were acquired on May 19th, 2011, October 5th, 2011 (Fig. 1b), January 22nd, 2012 and July 6th, 2012 (Fig. 1c). At the pre-processing stage, the images were co-registered with each other and calibrated to top of atmosphere (TOA) reflectance values.

For the training of the second-classification stage and for validation of the final output map, the reference data were collected during a European Life project (LIFE12 BIO/IT/000213) carried out to eradicate *A. altissima* invasive species (Casella et al., 2015a; Casella et al., 2015b; Casella et al., 2016).

2.4. Methodology

The classification system used consisted of a two-stage hybrid scheme. The first stage can provide an LC map from multi-seasonal VHR imagery without training reference data. The LC map can be used as a pre-filter to extract the deciduous vegetation layer to which the *A. altissima* species belongs. In the second stage, the invader pixels were distinguished from those belonging to other deciduous vegetation by

means of a *data-driven* classifier.

Specifically, the first stage of the classification system was based on an object-based (Ma et al., 2017), knowledge-driven LC classification algorithm within the eCognition framework (Trimble, 2014). The algorithm was developed in a previous study (Adamo et al., 2015; Lucas et al., 2015). It is based on multi-class discrimination using spectral and context rules provided through the elicitation of prior expert knowledge about: agricultural practices, class phenology, spectral and spatial features. The input to the first stage were the multi-seasonal WV-2 images available corresponding to: the biomass pre-peak (January); the biomass peak (May); the dry season (July); the biomass post-peak (October).

One of the critical steps of object-based classification is the selection of an appropriate segmentation scale for the identification of homogeneous objects in the image by means of a segmentation procedure. In order to provide classification outputs with different levels of detail, two different segmentation scales were used thus obtaining Small Object (SO) and Large Object (LO) segmentations (Lucas et al., 2015).

Using the biomass post-peak (October) image (R-G-B-NIR1 bands), the SO segmentation aggregated pixels into objects by considering spectral similarity only. The output segments, belonging to the small landscape components, appeared to be characterized by a small extension (e.g., tree crown scale). By using scale and shape indices (e.g., smoothness and compactness) along with spectral (R-G-B-NIR1bands) and texture homogeneity (1st order entropy) rules, LO segmentation provided large image segments (field scale). The resulting output segments represent macro structure and aggregations of the landscape. Thus, for *A. altissima* detection, the LO scale segmentation was not considered. Instead, the SO segmentation output map was used by applying expert rules for the subsequent classification phase. Thus, the multiple scale analysis can provide the selection of products more adequate for specific applications responding to different purposes.

The resulting Land Cover classified map (at the SO scale) was then used as input to the second classification stage of the hybrid system.

It is worth noting that no training data were needed to produce the output LC map by the hybrid system first stage. The classifier employed the same hierarchical scheme and taxonomy as the one adopted by the Food and Agriculture Organization Land Cover Classification System (FAO-LCCS) (Di Gregorio et al., 2005). The FAO-LCCS taxonomy provides a framework which, by integrating additional ancillary data, can be used to translate any LC class into different habitats (Tomaselli et al., 2013; Adamo et al., 2014; Lucas et al., 2015; Adamo et al., 2016; Gavish et al., 2018).

The natural deciduous vegetation layer to which *A. altissima* belongs was extracted from the LC map obtained as output of the first stage and this layer was used for the masking of the images to be analysed in the second stage. Initially, based on prior-knowledge, only the pixels of the natural deciduous class from the first stage were considered as input to the second stage. Then, based on misclassifications occurring between natural broadleaved deciduous vegetation and cultivated broadleaved vegetation evidenced by the PA values in the first-stage classification confusion matrix, the cultivated deciduous pixels were added into the deciduous vegetation layer considered as input to the second stage. The selection of the pixels belonging to the deciduous layer may have had an impact on the final classification map. In Murgia Alta, the broadleaved deciduous class is composed of both natural trees and shrubs vegetation and cultivated broadleaved vegetation (which consists mainly of orchard trees and vineyard shrubs).

The second stage of the algorithm was based on the well-known ML, a pixel-oriented, data-driven classifier which requires little input parameter tuning, has low computational costs and is easily accessible to any end-user. In consideration of its advantages, ML was adopted to rapidly assess how effective the use of a pre-filtering LC map could be for the production of accurate invasive species maps.

Fig. 2 schematises the hybrid two-stage classification algorithm adopted.

For training the supervised ML classifier, 5368 reference pixels were used to detect only two vegetation classes, namely *A. altissima* and other deciduous plants. Among the training reference pixels considered, 272 belonged to *A. altissima* and 5096 to other deciduous vegetation. An additional set of 8902 reference pixels was then selected from the in-situ data to validate the output map. Among these pixels, 845 belonged to *A. altissima* whereas 8057 belonged to other deciduous plants. Stratified random sampling was then applied to obtain a sample population that could best represent the entire population under study. Through this sampling technique, it was ensured that segments of the population were neither overrepresented, nor underrepresented (Congalton and Kass, 2009).

Moreover, in order to identify the minimum set of seasons to be analysed for *A. altissima* discrimination, different input configurations to the classifiers (reported in Section 3, Table 2, column 2) were considered by relying on prior-knowledge of species phenology.

Once the best configuration was found, first, the full set of the images spectral bands were used. Then, three spectral indices, generally used as a proxy of many vegetation related variables, were analysed to evaluate the results obtained with a reduced number of features.

It is worth noting that the spectral indices analysed do not cover the whole spectral range of the full band set (Section 2.3). The choice of not investigating further spectral indices may have had an impact on the classification performance. However, we think that it can be useful to quantify how low the system performance can get when less spectral regions are used.

The indices investigated in this study include the well-known Normalized Difference Vegetation Index (NDVI):

$$\mathrm{NDVI} = \frac{NIR1 - RED}{NIR1 + RED} \tag{1}$$

the Green Normalized Difference Vegetation Index (GNDVI):

$$\mathrm{GNDVI} = \frac{NIR1 - GREEN}{NIR1 + GREEN} \tag{2}$$

and the Modified Soil Adjusted Vegetation Index (MSAVI):

$$\mathrm{MSAVI} = \frac{2*NIR1 + 1 - \sqrt{((2*NIR1 + 1)^2 - 8*(NIR1 - RED))}}{2} \tag{3}$$

Specifically, the GNDVI is mostly used to determine water and nitrogen plant uptake into the crop canopy (Gitelson et al., 1996), whereas the MSAVI can maximize the reduction of soil effects on the vegetation signature. Soil effect reduction may be important when analysing VHR imagery (Qi et al., 1994).

The chosen spectral indices comparison can be justified considering on the one hand that end-users, not well acquainted with satellite data analysis and feature extraction, generally employ few indices (e.g. NDVI); on the other, that usually, data from VHR sensors, such as those from drones, include only BLUE, GREEN, RED and NIR bands. This comparison can provide a costs/benefits analysis. The two-stage classification hybrid system was applied to produce a reliable *A. altissima* map and to identify both small and larger areas invaded by this species (Section 3).

To improve the overall accuracy classification value obtained by the ML classifier, first a convolution median low-pass filter was applied to the output map. Then, the ML was substituted with an SVM classifier. The substitution was motivated by the fact that, even with small training samples, the SVM can yield better generalization performances even though requiring more computational effort and tuning of input training parameters than the ML classifier (Horvath, 2003; Foodya nd Mathur, 2004; Bruzzone and Persello, 2009; Mountrakis et al., 2011; Zheng et al., 2015; Belgiu and Drăguţ, 2016). Both a polynomial and an RBF kernel function were tested and compared. For comparison purposes with ML, the convolution median filter was applied also to the output of the SVM classifier.

All the different settings which were investigated can be justified by

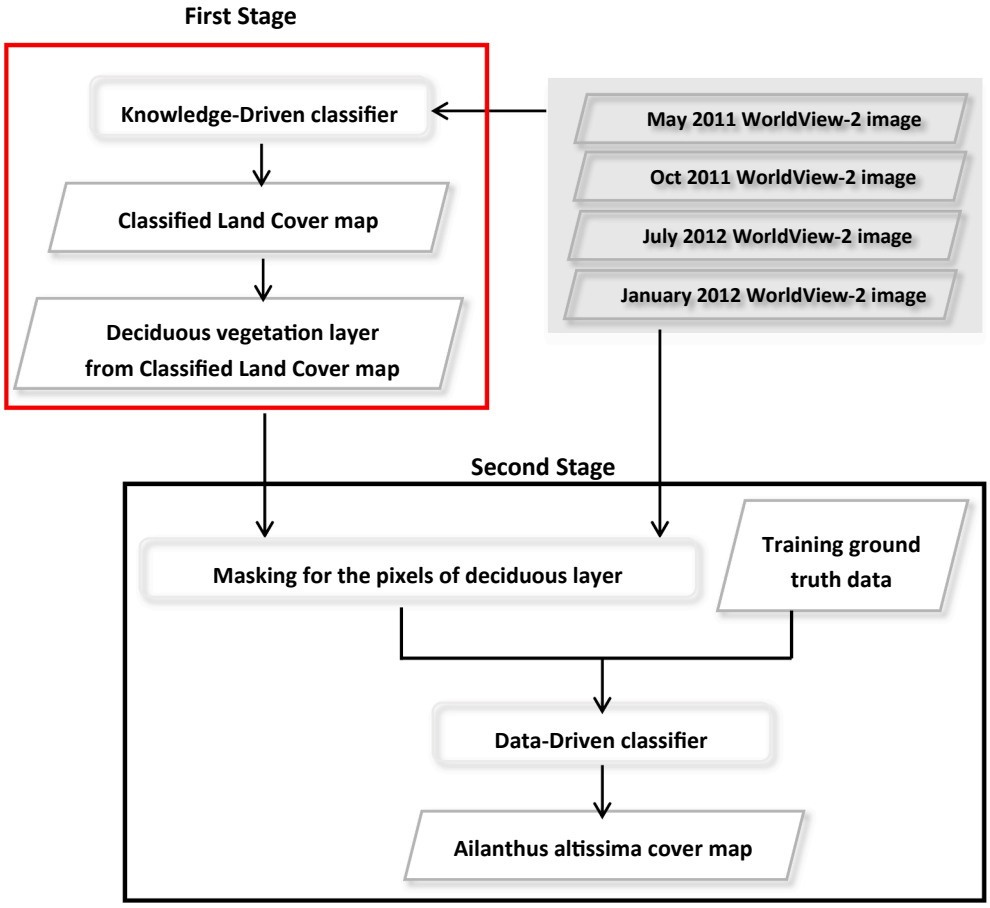

Fig. 2. Two-stage classification algorithm. Red rectangle, object-oriented, knowledge-driven first classification stage; black rectangle, pixel-oriented, data-driven second classification stage. Maximum Likelihood and Support Vector Machines classifiers were considered and their results compared in the second stage.

considering that the LC map of the first stage had been already optimized: (a) within the knowledge based approach of our work or, (b) by the map providers when considering an existing map (e.g., the ones produced through in-field campaigns by the protected area management authorities). Thus, an improvement of the final invasion map could be obtained by improving only the second classification stage.

The ENvironment for Visualizing Images (ENVI) framework, version 5.4, was adopted to perform all the classifications in the second stage (Harris Geospatial Solution). ENVI allows to, either easily select default input configuration parameters, or change them according to specific requirements, thus it can support even non-specialized users.

2.5. Accuracy assessment

The accuracy assessment protocol described in Olofsson et al. (2013; 2014) and Tarantino et al. (2016) was adopted in the second stage of the system. This protocol uses the information obtained from the traditional map confusion matrix (Congalton and Kass, 2009) to estimate the area of each LC class and to construct confidence intervals that reflect the uncertainty of the estimates obtained. In this framework, the sample error matrix is reported in terms of: (a) the unbiased stratified estimator of the proportion of area ($\hat{p}_{ij}$) in each cell *i,j* of the matrix; (b) OA, both UA and Producer's Accuracy (PA), with standard errors estimates (Section 4.3 in Olofsson et al., 2014). When map categories are reported as rows (*i*) and the reference categories are shown as columns (*j*), A_{tot} represents the total area of the map (window), $A_{m,i}$ is the mapped area (ha) of category *i* in the map and $W_i = \frac{A_{m,i}}{A_{tot}}$ is the proportion of the mapped area as category *i*, $\hat{p}_{ij}$ is then:

$$\hat{p}_{ij} = W_i \frac{n_{ij}}{n_{i\cdot}} \tag{4}$$

where n_{ij} corresponds to sample counts. The unbiased stratified estimator of the area of category *j* can be obtained as:

$$\hat{A}_j = A_{tot} \times \hat{p}_j = A_{tot} \sum_i W_i \frac{n_{ij}}{n_{i\cdot}} \tag{5}$$

where $\hat{A}_j$ can be viewed as an "error-adjusted" estimator of area because it includes the area of omission error of category *j* and leaves out the area of commission error.

The estimated standard error of the estimated proportion of area is:

$$S(\hat{p}_j) = \sqrt{\sum_{i=1}^{q} W_i^2 \frac{\frac{n_{ij}}{n_{i\cdot}}\left(1 - \frac{n_{ij}}{n_{i\cdot}}\right)}{n_{i\cdot} - 1}} \tag{6}$$

Finally, the standard error of the stratified area estimate can be expressed as:

$$S(\hat{A}_j) = A_{tot} \times S(\hat{p}_j) \tag{7}$$

and an approximate 95% confidence interval for A_j is:

$$\hat{A}_j \pm 2 \times S(\hat{A}_j) \tag{8}$$

2.6. Mc Nemar's test

Besides the aforementioned accuracy assessments, the significance of the performance discrepancies between pairs of classifiers adopted in the second classification stage (Bostanci and Erkan Bostanci, 2013) was

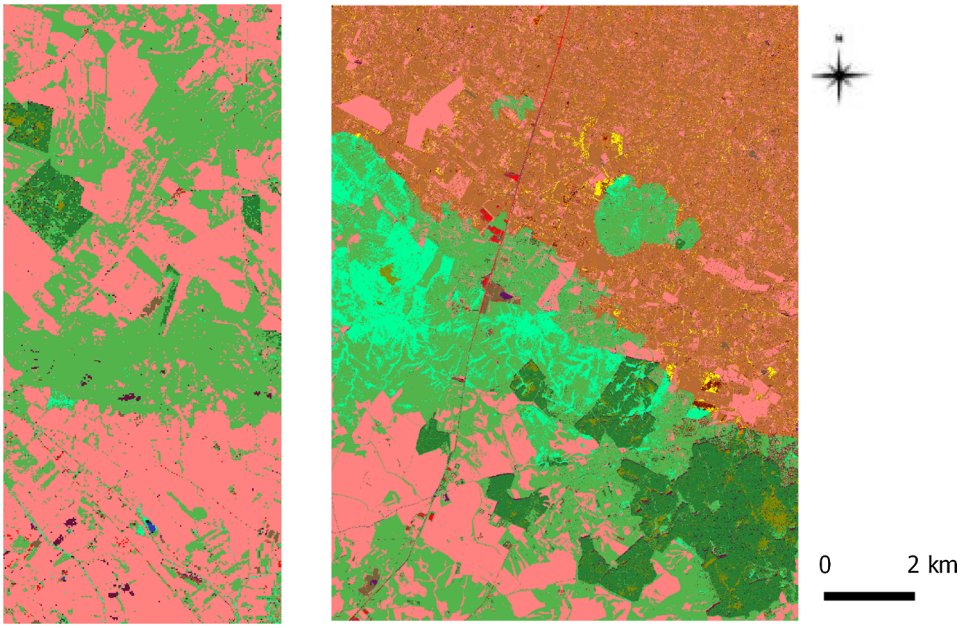

Fig. 3. Two sub-sets of the Land Cover map obtained by the knowledge driven classifier used in the first stage of the whole classification system (Fig. 2). (For interpretation of the references to colour in this figure legend, the reader is referred to the web version of this article.)

assessed using Mc Nemar's test. The latter is a variant of χ^2 test which consists of a non-parametric analysis by matching pairs of data from two algorithms. This matching produces four possible outcomes which can be arranged in a 2×2 contingency table. The performance discrepancies between the two algorithms can be evaluated on the basis of a z score, which is a function of the number of times one algorithm failed and the other succeeded. When $z = 0$, the two algorithms can be considered as providing similar performance. When the z value diverges from 0 in positive direction, it can be inferred that the performance of the two algorithms differs significantly.

3. Results

The hybrid system proposed in the present paper was applied to investigate the usefulness of multi-temporal VHR imagery in the detection of *A. altissima* invasive species, in Murgia Alta. Fig. 3 shows the LC map obtained as output of the system first-stage by analysing the 4 input multi-seasonal images available. This map includes 14 LC classes (Appendix A). As reported in the previous Section, only expert prior-knowledge was used to train the first-stage classifier (Adamo et al., 2015). In-situ reference data were instead used only to validate the output LC map with a resulting OA value of 92.77 ± 0.04%.

For the LC natural vegetation woody broadleaved, trees or shrubs, deciduous (A12/A1.A3 or A4.D1.E2) class, the UA and PA values obtained were 69.30% and 89.48%, respectively. The PA value (89.48%) derives from the fact that 7% of available reference natural deciduous pixels were misclassified as cultivated shrubs broadleaved deciduous class (A11/A2.A7.A10). In Murgia Alta, all the reference pixels of such class belong to vineyards. In addition, 3% of natural deciduous pixels were misclassified as cultivated trees or shrubs broadleaved deciduous (class A11/A1 or A2.A7.A10) belonging to fruit trees or shrubs in the area. Such low percentage values of misclassifications obtained along with prior-knowledge about species spreading (Section 2.2) support the choice of the natural deciduous layer only as input to the second classification stage for detecting *A. altissima* species. Nevertheless, once the best second stage setting was identified, the cultivated trees or shrubs deciduous pixels were included in the input deciduous layer to the second classification stage.

The UA value obtained (69.30%), indicates that 18%, 7% and 2% of the reference pixels from natural trees broadleaved evergreen, cultivated broadleaved shrubs (vineyards) as well as deciduous trees (orchard) classes, respectively, were misclassified as natural broadleaved deciduous. The findings show that an overestimation of the natural broadleaved evergreen pixels occurred in the LC map of the first classification stage.

In the LC map (Fig. 3), the natural broadleaved deciduous vegetation layer (A12/A1.A3 or A4.D1.E2) appears to be highly interconnected with the natural grassland ecosystem (i.e. herbaceous graminoids class, A12/A2.A6), whereas the cultivated broadleaved (trees and shrubs) deciduous vegetation (in the upper right corner of the image characterized by low digital elevation values) results to be well separated from natural grasslands.

Table 2 reports the results of the *A. altissima* mapping obtained from different second-stage input configurations. Each configuration is labelled with a different identifier (ID 1–11). ID 1 and ID 2 report the results obtained using all the spectral bands of the spring (May) and the summer (July) images which were analysed one image at the time. The OA and *A. altissima* UA values obtained for July (80.59 ± 0.34% and 37.32 ± 1.10%) were larger than the ones obtained for May (68.57 ± 0.31% and 22.64 ± 0.74%), respectively. Nonetheless, the July values can still be considered rather low, thus requiring the integration of additional data. For this purpose, image pairs from July–January (ID 3), July–May (ID 4) and July–October (ID 5) were analysed.

When using the July-January image pair, better OA (84.76 ± 0.39%) and UA (50.93 ± 1.26%) values were obtained (ID 3). From Table 2, it can be observed that the July-May image pair (ID 4) provided OA and UA values smaller than the ones reported in IDs 2 and 3, respectively. When the multi-spectral stack of the July-October pair was analysed, the identification of *A. altissima* pixels improved significantly, with an increase of both OA (90.51 ± 0.27%) and UA (55.05 ± 1.29%) values (ID 5).

Although the application of a filtering procedure may remove not only noisy and false positive pixels, but also some pixels belonging to isolated *A. altissima* plants, a median filter was adopted to improve the final UA an OA values (Haralick et al., 1987). This choice increased the OA and UA values up to 99.20 ± 0.07% and 79.15 ± 1.61%, respectively, for a 5x5 window size. As expected, the *A. altissima* mapped area (A_m) value and the stratified area estimate, with 95% confidence interval, were not only the smallest values (ID 5), but also resulted quite

Table 2
Results obtained from 2nd stage different input configurations. Each configuration is labelled with a specific Identifier (ID) in the table. UA, PA as well as OA values (%) are provided with standard errors (Olofsson et al., 2014).

Error matrix: *A. altissima* vs. *Other Deciduous Vegetation*									
ID	**Input configuration to the 2° stage**	**Classifier**	***A. altissima* UA**	***A. altissima* PA**	***Other* UA**	***Other* PA**	**OA%**	**Am (ha) Mapped Area *A. altissima***	**Stratified *A. altissima* Area Estimate 95% Conf. Interv. (ha)**
1	May	ML	22.64 ± 0.74	87.93 ± 0.98	98.01 ± 0.19	66.40 ± 0.39	68.57 ± 0.31	527.56	135.85 ± 8.34
2	July	ML	37.32 ± 1.10	89.76 ± 1.11	98.26 ± 0.16	79.33 ± 0.32	80.59 ± 0.34	391.63	162.82 ± 9.11
3	July and January	ML	50.93 ± 1.26	97.17 ± 0.75	99.36 ± 0.09	82.44 ± 0.28	84.76 ± 0.39	407.01	213.31 ± 10.43
4	July and May	ML	31.60 ± 0.94	94.61 ± 0.82	98.97 ± 0.13	71.74 ± 0.35	74.51 ± 0.35	490.39	163.79 ± 9.43
5	July and October	ML	**55.05 ± 1.29**	**97.49 ± 0.58**	99.64 ± 0.07	89.60 ± 0.28	**90.51 ± 0.27**	347.48	196.19 ± 9.16
		after filtering: 3 × 3	68.46 ± 1.48	94.03 ± 0.74	99.60 ± 0.07	97.15 ± 0.21	96.95 ± 0.14	106.27	77.37 ± 3.55
		5 × 5	79.15 ± 1.61	87.80 ± 0.81	99.72 ± 0.06	99.46 ± 0.14	99.20 ± 0.07	30.08	27.12 ± 1.70
6	July, January, May, October	ML	53.64 ± 1.27	98.91 ± 0.50	99.73 ± 0.06	82.45 ± 0.27	85.26 ± 0.40	424.16	230.04 ± 10.84
7	NDVI: July and October	ML	26.78 ± 1.07	55.40 ± 1.53	94.66 ± 0.27	83.93 ± 0.28	81.20 ± 0.30	267.97	129.55 ± 8.10
8	GNDVI: July and October	ML	24.59 ± 0.99	40.08 ± 1.61	94.96 ± 0.26	90.19 ± 0.32	86.48 ± 0.26	162.73	99.84 ± 7.00
9	MSAVI: July and October	ML	46.67 ± 1.53	48.27 ± 1.45	95.93 ± 0.22	95.67 ± 0.23	92.22 ± 0.24	101.71	98.34 ± 6.39
10	July	SVM (RBF)	69.08 ± 1.66	45.81 ± 1.26	96.53 ± 0.20	98.66 ± 0.15	95.41 ± 0.21	55.00	82.95 ± 5.57
11	July and October	SVM (RBF)	**82.47 ± 1.32**	**61.16 ± 0.99**	98.42 ± 0.14	99.47 ± 0.14	**97.96 ± 0.14**	39.46	53.22 ± 3.77
		after filtering: 3 × 3	94.85 ± 0.93	11.39 ± 0.60	98.77 ± 0.21	99.97 ± 0.05	98.26 ± 0.21	6.79	56.56 ± 5.57
		5 × 5	97.47 ± 0.01	3.84 ± 0.10	99.40 ± 0.25	100.00 ± 0.01	99.41 ± 0.25	3.01	78.49 ± 6.70
12	July and October	SVM (Polynomial; degree: 2)	82.13 ± 1.33	60.16 ± 0.99	98.38 ± 0.14	99.46 ± 0.14	97.91 ± 0.14	39.00	53.25 ± 3.83
13	July and October. Input layer includes natural and cultivated broadleaved deciduous	SVM (RBF)	82.77 ± 1.31	64.22 ± 1.05	98.04 ± 0.15	99.26 ± 0.13	97.42 ± 0.16	55.00	70.89 ± 4.24

similar after filtering (5 × 5).

When the four-seasonal spectral stack was used as input to the second stage (ID 6), the UA and OA values (53.64 ± 1.27% and 85.26 ± 0.40%, respectively) resulted lower than the ones obtained from the July-October image pair (55.05 ± 1.29% and 90.51 ± 0.27%, respectively).

In order to test final classification accuracy with LC map and without LC map, the two-classes (*A. altissima* and other deciduous vegetation) available ground truth information was used to train a single stage supervised ML classifier. When using the four WV-2 images available, the results obtained by a single stage supervised ML classifier, without pre-filtering, evidenced a decrease in the UA and OA values (53.50 ± 1.27% and 55.54 ± 1.21%, respectively) and a very large *A. altissima* mapped area (47259.84 ha). Instead, when using the July-October image pair only, the UA and OA values were slightly larger than the previous ones (55.68 ± 1.30% and 64.07 ± 1.05%, respectively) with a lower *A. altissima* mapped area (39966.40 ha). Such high values for the *A. altissima* mapped area value, with respect to the corresponding (not filtered) two-stage *A. altissima* mapped area results (424.16 ha, ID6), indicates that most of the image pixels were misclassified as *A. altissima*. These findings confirm the usefulness of the two-stage approach.

In a further ML classification experiment, only vegetation spectral indices from the bi-temporal (July-October) data set were used as input. When the NDVI index from the July-October image pair was used as input to the second stage, no improvement of the OA was noticed (ID 7). The OA value (81.20 ± 0.30%) remained lower respect to the bi-temporal stack (ID5), while the UA resulted very low (26.78 ± 1.07%).

For comparison purposes, two additional vegetation indices, i.e., the GNDVI (ID 8) and MSAVI (ID 9), were applied to the same image-pair. Among the indices investigated, the results reported in IDs 8 and 9 indicate that MSAVI provided the largest OA (92.22 ± 0.24%) value, but a lower UA (46.67 ± 1.53%) with respect to the bi-temporal stack (ID 5).

Table 3 shows the results obtained by applying McNemar's test to pairs of classifiers which correspond to different algorithms or input configurations. This step was intended to assess the statistical significance of the different OA values obtained.

Figs. 4–6 show four close-up images extracted from the final output map obtained from the July-October image pair. These images provide samples of the detection of true invasive pixels.

Fig. 7a–c, represent close-up of the final output map obtained from three different second-stage input configurations, namely July–January (ID 3), July–May (ID 4) and the whole multi-seasonal data set (ID 6), respectively. In these maps, *A. altissima* pixels, shown in the red polygon areas, were proved false by in-field validation campaigns. The pixels in questions were not detected in the July–October output map, Fig. 7d. This result appears to be in agreement with the well-known fact that *A. altissima* species can hardly grow in dense woodland areas as the ones surrounding the zone investigated (Fig. 7e).

Drawing on the aforementioned results, the July image (ID 10) and the bi-temporal July-October image pair (ID 11 and ID 12) were used separately as input to the SVM classifier. In the second stage the SVM substituted the ML classifier for performance comparison.

When the Radial Basis Function (RBF) with the SVM default parameters i.e., penalty C = 100 and kernel function $\gamma = 0.063$, proposed by ENVI tool, were used for the single-date image, SVM analysis (ID 10) provided larger OA and UA values (95.41 ± 0.21% and 69.08 ± 1.66%) than the ones obtained through ML (80.59 ± 0.43% and 37.32 ± 1.10%, respectively). For the July–October image pair, the OA (97.96 ± 0.14%) obtained was quite comparable with the one from the ML (99.20 ± 0.07%) following the application of a 5 × 5 filter. For tuning the SVM configuration parameters, various C and γ pairs were tested, but no significant changes in the classification results were achieved. Similar OA and UA values (97.91 ± 0.14% and 82.13 ± 1.33%) were obtained when the polynomial SVM kernel

Table 3
Results obtained by applying Mc Nemar's test to selected pairs of classifiers used in the second stage (Table3a). The arrowheads (←, ↑) denote which classifier performed better in the given datasets. Z scores are given next to the arrowheads as a measure of how statistically significant the performances of the compared classifiers are. The contingency tables obtained for the classifier pair SVM and ML before and after filtering (5 × 5), using 2 seasons as input to both classifiers, are reported in Table 3b and Table 3c. In such Tables, A and OD labels indicate *A. altissima* and Other Deciduous pixels, respectively, as components of the total number of failed or succeeded pixels reported in the Tables.

(a)	ML input: 2 seasons	ML input: 2 seasons after filtering (5 × 5)	ML input: 4 seasons	ML input: MSAVI
ML input: 2 seasons		↑7.36	←1.84	
ML input: NDVI				↑16.4
SVM input: 2 seasons	←14.43	←7.11		

(b)		ML	Z = 14.43
		Failed	**Succeeded**
SVM	**Failed**	169 (27 A + 142 OD)	135 (131 A + 4 OD)
	Succeeded	526 (0 A + 526 OD)	8072 (687 A + 7385 OD)

(c)		ML5 × 5	Z = 7.11
		Failed	**Succeeded**
SVM	Failed	109 (71 A + 38 OD)	282 (87 A + 195 OD)
	Succeeded	633 (269 A + 364 OD)	8234 (418 A + 7816 OD)

function was used (ID 12).

The application of the median filter (5 × 5 size) to the SVM classifier improved the UA and OA values up to 97.47 ± 0.01% and OA = 99.41 ± 0.25%. However, as expected, this filter application drastically reduced the PA to 3.84 ± 0.10%, with loss of most of the reference pixels.

When cultivated broadleaved deciduous pixels were added to the natural deciduous pixels, as input of the SVM classifier, the UA and OA values did not change with respect to the one obtained by the natural deciduous pixels alone. Only a slight increase in the PA (from 61.16 ± 0.99% to 64.22 ± 1.05%) was obtained.

Fig. 8a and b report the results of the ML and SVM classifications in one window of the output image. In particular, Fig. 8a shows a deciduous oak tree which was classified as *A. altissima* by the ML, whereas the plant was correctly recognized as other deciduous plant by the SVM.

4. Discussion

The findings reported in the present study encourage the use of both VHR imagery and the hybrid classification approach proposed for *A. altissima* invasive species mapping. The results presented in Table 3, related to Mc Nemar's statistical test, evidence the statistical significance of the performance differences resulting from the configuration pairs investigated.

4.1. Best season and filtering evaluation

The mapping carried out with single-date WV-2 imagery reveals that the image acquired in July can discriminate *A. altissima* plants better than the image acquired in May (Table 2). This finding is consistent with the results reported by Burkholder et al. (2011) who obtained the lowest error in the July spectra. However, it seems worth noting that, Burkholder et al. (2011) investigated laboratory spectra of *A. altissima* leaves collected from May to August in a site in West Virginia, whereas our study concerned satellite WV-2 data classification of *A. altissima* in Murgia Alta, a site in the Mediterranean basin.

Our results indicate that, when only the July image was used as input to the second-stage classification, the UA, PA and OA values obtained by the ML classifier were lower than when using bi-seasonal images. Actually, the best results (UA = 55.05 ± 1.29%; PA = 97.49 ± 0.58% and OA = 90.51 ± 0.27%) were achieved when the October (autumn) image was added to the July one and the whole bi-temporal WV-2 spectral stack was analysed (Table 2). This finding could be related to the *A. altissima* phenology, which differs from other deciduous plants growing in Murgia Alta.

In this site, the *A. altissima* leaves start to turn yellow at the end of September and, depending on temperature, they can be completely lost by the end of October. Other trees, such as wild pear and oak trees (i.e., *Quercus pubescens*) distributed on the area, exhibit delayed time in their phenology (Casella et al., 2016). This characteristic may have influenced the results of our study.

By employing a low-pass median filtering, the UA and OA values obtained by the ML from July-October stack increased up to 79.15 ± 1.61% and 99.20 ± 0.07%, respectively (Table 2). However, the PA decreased from 97.49 ± 0.58% to 87.80 ± 0.81% as a consequence of true pixels loss due to filtering. When the Mc Nemar's test was applied to the ML classifier before and after filtering (5 × 5 size), the significance of the filter performance was evidenced (z = 7.36). The filter reduced the overestimation of *A. altissima* pixels (Table 3). The ML classification involved low parameter complexity and low computational costs, but it lost true *A. altissima* pixels.

As evidenced by the low value obtained by Mc Nemar's test (z = 1.84), the use of full four-seasonal spectral stack introduced no significant improvement in the classification performance than when using the bi-temporal stack. This finding suggests that, when an LC map is already available and there is no need to run the first classification

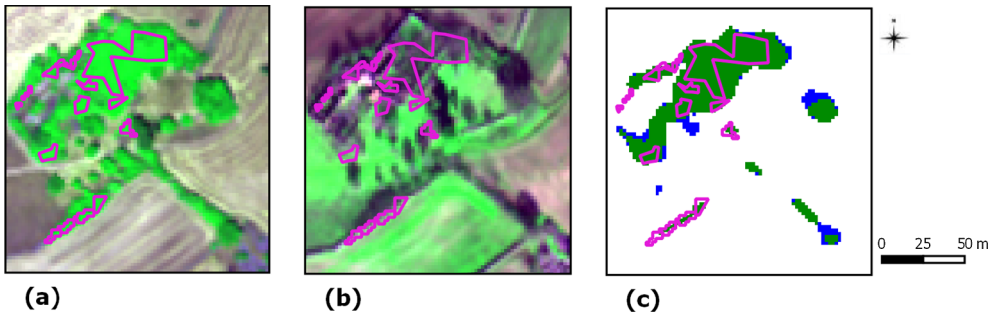

Fig. 4. Close-up 1: (a) WV-2 July and (b) WV-2 January images, False Colour Composite: Band 5, Band 7, Band 2. Deciduous plants can be observed. (c) *A. altissima* (5 × 5) filtered ML output map from second stage using the July–October image pair as input. In-field polygons of *A. altissima,* used for validation, are highlighted in magenta line.

stage, only two VHR images, one of summer and the other of autumn, need to be collected for *A. altissima* mapping.

4.2. Feature reduction

The last ML classification experiment was carried out by using only NDVI, GNDVI and MSAVI vegetation indices which were extracted from the July-October bi-temporal stack. The results show that among the vegetation indices used, MSAVI can provide the highest UA and OA values, i.e., 46.67 ± 1.53% and 92.22 ± 0.24%, respectively (Table 2). This finding was also confirmed when using the Mc Nemar's test (z = 16.4) to compare MSAVI and NDVI results (Table 3). The data obtained confirm the importance of reducing the impact of soil signature when analysing VHR data (i.e., WV-2) through the MSAVI.

When using MSAVI, however, lower UA and PA accuracy values were obtained, from the same input July-October image pair, respect to the whole bi-temporal band stack. This result may have been due to the fact that the indices considered related only to some spectral bands (i.e., RED, GREEN, NIR1). Undoubtedly, wider selection of vegetation indices would have been required in order to optimize computational costs and performances. However, since the main objective of this study is to evaluate the effectiveness of multi-spectral VHR imagery for *A. altissima* mapping, both investigation and comparison of additional spectral indices remain remote to the scope of our study.

The foregoing discussion leads to the suggestion that the use of the whole spectral information available from multi-spectral satellite imagery can support end-users to solve vegetation related issues adequately when a dedicated index selection cannot be carried out. Our observation, about the need to use the whole band set available for *A. altissima* mapping, is in consonance with Tarantino et al. (2012) and Omer et al. (2015), even though these studies used no index and based their conclusions on the analysis of the different spectral bands of one image only.

Other studies, which focuse on hyperspectral data, have analysed in depth the selection of spectral indices. For instance, Groβe-Stoltenbeg et al. (2016) and (2018) have provided interesting details on the distribution of *Acacia longifolia* species in a Mediterranean dune ecosystem region. In the 2016 paper, the authors used field spectra data while in the 2018 one, they employed aerial hyperspectral imagery combined with LIDAR data.

In the 2018 paper, the authors reduced the spectral features by selecting 15 vegetation indices covering the full spectral range of the data considered. They reported the best result when fusing such vegetation indices with LIDAR data. In addition, they validated the effectiveness of a new index, namely the Near Infrared Vegetation Index, which can be related to the Gross Primary Production and seems able to evaluate the impacts of invasive species on ecosystem productivity (Groβe-Stoltenbeg et al., 2018).

4.3. Second stage: classifiers comparison

In the present study, the best results for both the single July image and the July-October image pair were achieved when the SVM classifier was adopted in the second stage. For the image pair, the significance of the performance difference between the SVM and ML (without filtering) classifiers, was confirmed by the high value of the Mc Nemar's test ($z = 14.43$) reported in Table 3a. In light of the comparison between SVM and ML (before and after filtering) when using 2 seasons as input, for both classifiers, the data reported in Table 3b and 3c present the number of times when: either (1) both algorithms failed (left-top) or (2) succeeded (right, bottom); or else (3) one of the algorithm failed and the other succeeded (right-top and left-bottom) considering the comparison of SVM and ML. Actually, most of *A. altissima* false positive pixels (526 of 845) obtained by the ML were correctly classified by the SVM as other deciduous (Table 3b).

When comparing the SVM performances with the ML ones, after filtering (5 × 5 size), a lower, but still significant, Mc Nemar's test value ($z = 7.11$) was obtained (Table 3a). This decrease may have been due to the reduction of false positive pixels obtained through the filtering. A loss of 364 out of 845 reference *A. altissima* pixels is evident in Table 3c.

The application of the median filter to the SVM output map lost most of the true *A. altissima* reference pixels, with a decrease of the PA value (from 61.16 ± 0.99% to 3.84 ± 0.10%), as reported in Table 2 (ID11). This finding can be due to the fact that the SVM classifiers can perform better than ML also when trained with limited reference

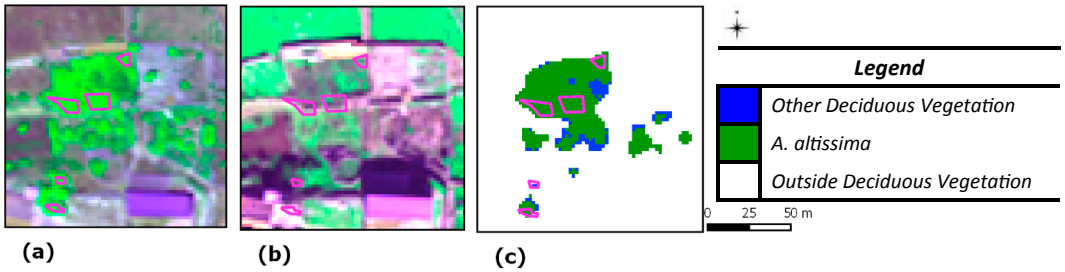

Fig. 5. Close-up 2: (a) WV-2 July and (b) WV-2 January images, False Colour Composite: Band 5, Band 7, Band 2. Deciduous plants can be observed. (c) *A. altissima* (5 × 5) filtered ML output map from second stage using the July–October image pair as input. In-field polygons of *A. altissima,* used for validation, are highlighted in magenta line.

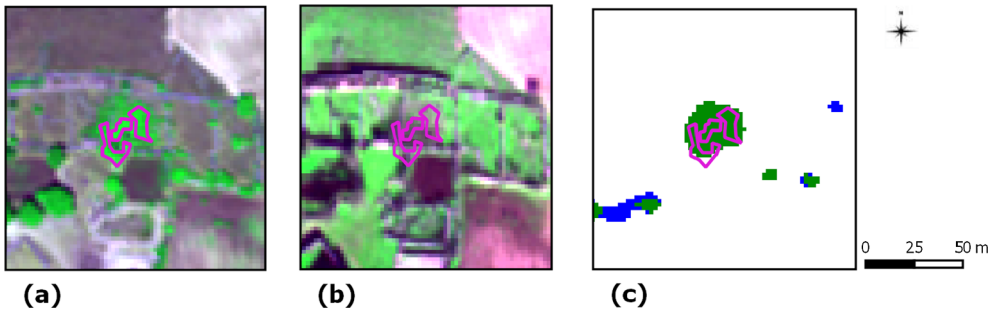

Fig. 6. Close-up 3: (a) WV-2 July and (b) WV-2 January images, False Colour Composite: Band 5, Band 7, Band 2. Deciduous plants can be observed. (c) *A. altissima* (5 × 5) filtered ML output map from second stage using the July–October image pair as input. In-field polygons of *A. altissima,* used for validation, are highlighted in magenta line.

ground truth (Atkinson et al., 2014).

The integration of both natural and cultivated broadleaved deciduous pixels, instead, provided a slight increase in the PA value (64.22 ± 1.05%), as reported in Table 2 (ID 13). This result may have been due to the identification of additional *A. altissima* pixels on the border of cultivated trees (orchard) and shrubs (vineyards) fields and evidences the impact of the first stage LC map on the second stage.

4.4. Comparison with other studies

Obviously, the results reported in the present study and those summarized in Table 1 cannot be directly compared. The findings of our study were obtained in a different geographical area and by means of a hybrid technique applied to analyse bi-temporal image stacks.

Specifically, Müllerova et al. (2017b) acquired multi-temporal Pleiades and UAV images for the mapping of *Fallopia japonica* invasive species in the Czech Republic, but analysed the images only on a monthly basis. Their study reports that, depending on the month analysed, the performance of the SVM was not always larger than the one obtained from ML. In (Müllerova et al., 2017b), the same authors report a better performance of ML respect to SVM when analysing both single date WV-2 and UAV imagery for the mapping of *Robinia pseudoacacia* species in the Czech Republic.

Comparison between the results reported by these authors and those presented in our study can hardly be made. The results presented by them were obtained from mono-temporal analysis while no mention of classifier error is available in their discussion.

The two studies, reported in Table 1, which include *A. altissima* mapping, differ respect to ours in regard to the number of species, input data, techniques and study area. In particular, Da Luz and Crowley (2010) identify the presence of *A. altissima* in comparison to that of 49 other invasive species in a site located in Virginia. In their study, the authors use hyperspectral Sebass airborne sensor and provide a ranking matrix for each species discrimination without mentioning OA measurements. Dvorak et al. (2015) use multi-spectral drone-based data to discriminate four classes of invasive plants, among which *A. altissima* in the Czech Republic, but report no quantitative evaluation of *A. altissima.* Therefore, the results reported in both papers do not allow quantitative comparison with our findings.

Even though the comparison between the data in Table 1 and the results of our study can hardly be made, the best OA value of 97.96 ± 0.14% was achieved in our study for *A. altissima* detection in

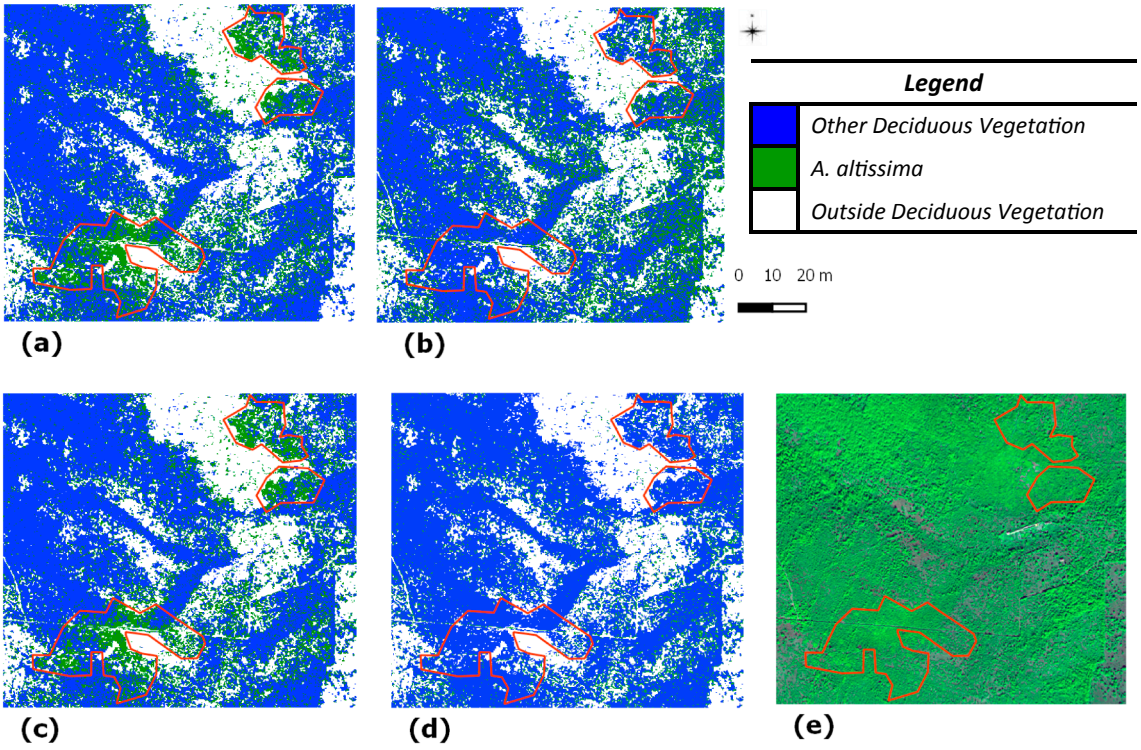

Fig. 7. Close-up 4: red polygonal areas evidence false *A. altissima* pixels in the maps originated by using as input to the second stage: (a) July–January pair; (b) July–May pair; (c) multi-seasonal July, January, May and October set. (d) The same pixels are correctly labeled in the map from July–October pair. The original WV-2 October input image is shown in (e) where the green area corresponds to mixed forest, on the ground. False Colour Composite: Band 5, Band 7, Band 2.

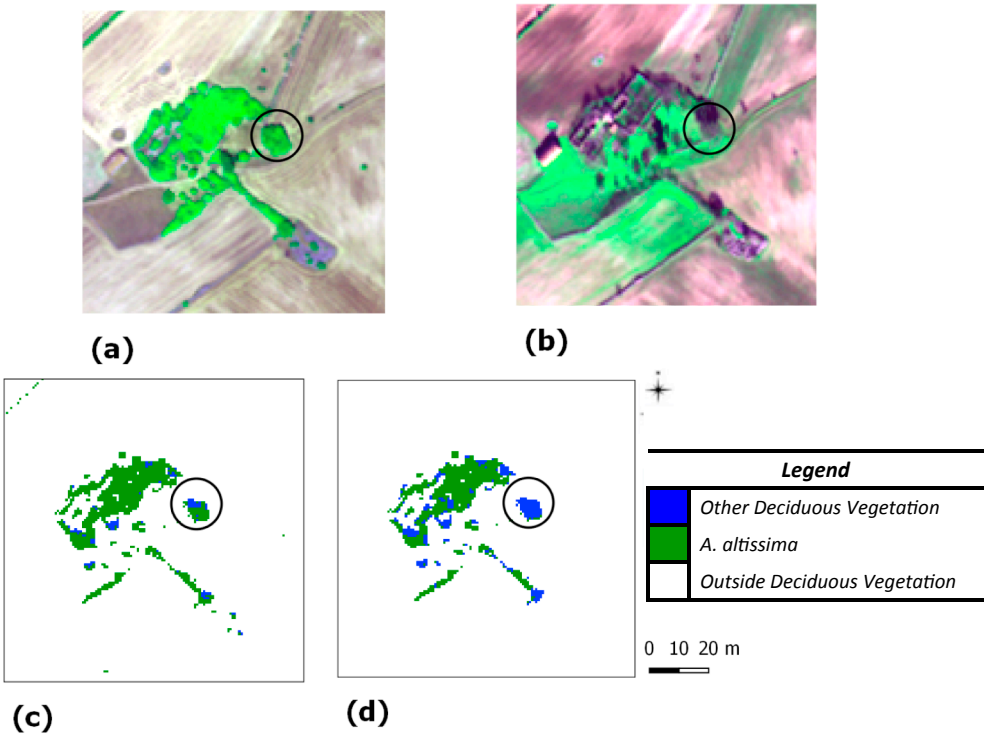

Fig. 8. Close-up 5 of (a) the July input image; (b) the January input image. False Colour Composite: Band 5, Band 7, Band 2. (c) The classified image obtained from ML; (d) the classified image obtained from SVM using the image pair July–October as input. The black circle evidences a deciduous oak tree in all figures. The tree was misclassified as *A. altissima* by the ML classifier.

Mediterranean region with VHR imagery. On the one hand, this result may be due to the hybrid technique used; on the other it may depend on the bi-temporal analysis carried out. In fact, when considering VHR data, excepting Niphadkar et al. (2017), all other studies mapped invasive species through the analysis of only mono-temporal imagery (Everitt et al., 2005; Peerbhay et al., 2016; Monteiro et al., 2017; Müllerova et al., 2017a; 2017b). In Table 1, among the studies using multi-spectral High Resolution imagery (e.g., Landsat, Sentinel-2), only Gavier-Pizarro et al. (2012) used multi-temporal data, whereas De Sá et al. (2017) acquired multi-temporal Landsat images to detect changes in *Acacia longifolia* spreading, but analysed only one date (November 2013) for the mapping of this species.

Our study indicates that multi-temporal VHR data can be adequate for *A. altissima* discrimination and monitoring in the Mediterranean region. Multi-temporal analysis can prove effective since it can exploit phenological information useful for discriminating species having spectral signature similar to other species detected in mono-temporal analysis. Even though WV-2 includes the RED EDGE band, it lacks SWIR bands and fine spectral resolution. As a result, the analysis of a single image can hamper species discrimination.

To reduce the number of VHR images involved in the multi-temporal analysis as well as to decrease related costs, accurate selection of the most significant seasons (and image) requires prior-knowledge of the climate and periodic biological phenomena (e.g., plant flowering) of the studied species.

4.5. Final suggestions

It seems worth recalling that VHR data are acquired only on demand, that no systematic historic archive of acquisitions are available as well as that regular use by public bodies and decision makers is still hampered by high acquisition costs. In consideration of these issues, Blonda et al. (2013) and Turner et al. (2015) have suggested that in order to reduce VHR costs for supporting frequent monitoring of easily growing invasive species, policy agreements between space agencies and national authorities should be encouraged and free access to VHR data should be guaranteed at least to public bodies (e.g. Protected Areas management authorities). In addition, VHR data, with at least one image per season, should be regularly acquired on the network of Protected Areas. When combined with other information these data could provide multi-scale regular monitoring of the conservation status of the endangered areas. The availability of a large amount of VHR data may contribute to cost reduction.

5. Conclusions

On-going climatic and anthropic changes are making invasive species spreading a global issue whose monitoring and management would require powerful remote sensing data and techniques, like the ones proposed in our study. The results of *A. altissima* mapping in the Murgia Alta protected site show that multi-spectral VHR satellite data can discriminate such a problematic species across large areas, especially when hyperspectral data from aerial campaigns are unavailable.

One of the advantages of the two-stage hybrid classification system proposed is that no ground reference multi-class data are required in the first stage, whereas in the second, reference ground data for only two classes, namely *A. altissima* versus other deciduous plants, are needed. Another advantage of the hybrid system is that when an updated LC map is available, the deciduous vegetation layer can be extracted from such a map and used, along with the two images, as input to the second stage. Thus, since only two VHR images need to be acquired, the technique allows data collection cost reduction.

The availability of Sentinel-2 multi-spectral images, which are collected with high spatial resolution (10–30 m), every 5 days, could further reduce the costs of invasive species mapping since these data are provided for free by the European Space Agency (ESA Sentinel online). Even though the spatial resolution of Sentinel-2 data may fail to detect single invasive trees, due to the possible exploitation of hyper-temporal information, such data may represent an additional opportunity for early detection of invasive species.

The results presented in our study may be considered limited since they relate to the mapping of *A. altissima* in a single study site of the Mediterranean region. Obviously, for the findings to be generalized, the methodology proposed and the data used would require further

application for the mapping of *A. altissima* and other invasive species in different sites. Pending more extensive applications, the results obtained through the hybrid approach can, on the one hand, provide a significant contribution towards the operationalization of the procedure, on the other, it can favour early species detection. In other words, compared to other supervised techniques, the approach employed in this study may open new options for the monitoring of invasive plants in many areas.

Acknowledgments

This work was supported by the European Union's Horizon 2020 Research and Innovation Programme, within the project ECOPOTENTIAL: improving future ecosystem benefits through earth observations, grant agreement 641762 (www.ecopotential-project.eu).

VHR images were provided by the European Space Agency data warehouse policy, within the FP7 BIO_SOS project (www.biosos.eu), grant agreement 263455. *A. altissima* reference ground truth data were collected within the Life Alta Murgia project LIFE12 BIO/IT/000213 (http://lifealtamurgia.eu/en/).

The authors are grateful to Prof. Maria Tarantino, for the patient reviewing of the English version of the paper.

Appendix A. Supplementary material

Supplementary data to this article can be found online at https://doi.org/10.1016/j.isprsjprs.2018.11.013.

References

Adamo, M., Tarantino, C., Tomaselli, V., Kosmidou, V., Petrou, Z., Manakos, I., Lucas, R.M., Mücher, C.A., Veronico, G., Marangi, C., De Pasquale, V., Blonda, P., 2014. Expert knowledge for translating land cover/use maps to general habitat categories (GHC). Landscape Ecol. 29, 1045–1067.

Adamo, A., Tarantino, C., Lucas, R.M., Tomaselli, V., Sigismondi, A., Mairota, P., Blonda, P., 2015. Combined use of expert knowledge and earth observation data for the land cover mapping of an Italian grassland area: an EODHAM system application. IEEE Geoscience and Remote Sensing Symposium. 3065–3068. ISBN: 978-1-4799-7929-5.

Adamo, M., Tarantino, C., Tomaselli, V., Veronico, G., Nagendra, H., Blonda, P., 2016. Habitat mapping of coastal wetlands using expert knowledge and Earth observation data. J. Appl. Ecol. 53, 1521–1532. https://doi.org/10.1111/1365-2664.12695.

Andrew, M.E., Ustin, S.L., 2008. The role of environmental context in mapping invasive plants with hyperspectral image data. Remote Sens. Environ. 112 (12), 4301–4317.

Atkinson, J.T., Ismail, R., Robertson, M., 2014. Mapping bugweed (*Solanum mauritianum*) infestations in *Pinus patula* plantations using hyperspectral imagery and support vector machines. IEEE J. Select. Top. Appl. Earth Observ. Remote Sens. 7, 17–28.

Bardsley, D.K., Edwards-Jones, G., 2007. Invasive species policy and climate change: social perceptions of environmental change in the Mediterranean. Environ. Sci. Policy 10, 230–242.

Belgiu, M., Drăguţ, L., 2016. Random forest in remote sensing: a review of applications and future directions. ISPRS J. Photogramm. Remote Sens. 114, 24–31.

Bostan, C., Borlea, F., Mihoc, C., Beceneaga, A.M., 2014. Spread species A. altissima in new areal and impacts on biodiversity. Res. J. Agric. Sci. 46, 104–108.

Bostanci B., Erkan Bostanci E., 2013. In: Bansal, J.C., Singh, P., Deep, K., Pant, M., Nagar, A.K. (Eds.), Proceedings of Seventh International Conference on Bio-Inspired Computing: Theories and Applications (BIC-TA 2012), Advances in Intelligent Systems and Computing. Springer, India. doi: 10.1007/978-81-322-1038-2_2.

Blonda, P., Lucas, R.M., Inglada, J., Stutte, J., Manakos, I., Dimopoulos, P., Lang, S., Corbane, C., Buck, O., Schöder, C., Vanden Borre, J., 2013. Copernicus Biodiversity Monitoring Services: the FP7 SPACE projects perspective-White Paper. < www.biosos.eu/publ/White_Paper_Biodiversity_Monitoring_BIOSOS_MSMONINA.pdf > .

Bradley, B.A., 2014. Remote detection of invasive plants: a review of spectral, textural and phenological approaches. Bio. Invasions. 16, 1411–1425.

Bruzzone, L., Persello, C., 2009. A novel context-sensitive semisupervised SVM classifier robust to mislabeled training samples. IEEE Trans. Geosci. Remote Sensing 47 (7), 2142–2154.

Burkholder, A., Warmer, T.A., Culp, M., Landenberger, R., 2011. Seasonal Trends in separability of leaf reflectance spectra for A. *altissima* and four other tree species. Photogramm. Eng. Remote Sens. 77, 793–804.

Casella, F., Vurro, M., 2013. *Ailanthus altissima* (tree of heaven): spread and harmfulness in a case-study urban area. Arboricultural J.: Int. J. Urban Forestry 35 (3), 172–181.

Casella, F., Boari, A., Zonno, M.C., Palomba, G., Vurro, M., 2015a. Control of A. altissima in a natural environment. In: Proceedings of 17th European Weed Research Society Symposium "Weed management in changing environments", Montpellier, France, 23–26 June, 246.

Casella, F., Vurro, M., Palomba, G., 2015b. Presenza di A. altissima nel Parco Nazionale dell'Alta Murgia: risultati della mappatura eseguita nell'ambito del Progetto "Life Alta Murgia". In: Proceedings of the International Conference "Management and conservation of dry grasslands in Natura 2000 sites", Rome, Italy, 26–27 March, 28–30.

Casella, F., Vurro, M., Boari, A.G., 2016. Restoration of areas infested by A. altissima in the Alta Murgia National Park: experience within a LIFE project. In: Proceedings of the 7th International Weed Science Congress, Prague, Czech Republic, 19–25 June, 215.

Celesti-Grapow, L., Pretto, F., Carli, E., Blasi, C., 2010. Flora vascolare alloctona e invasiva delle regioni d'Italia. In: Celesti-Grapow, L., Pretto, F., Carli, E., Blasi, C. (Eds.), Casa Editrice Universitaria La Sapienza, Rome, Italy.

Congalton, R. G., Kass, G., 2009. Assessing the accuracy of remotely sensed data: principle and practices. second ed. CRC Press/Taylor & Francis Group. ISBN 9781420055122.

Council Directive 92/43/EEC < http://eur-lex.europa.eu/legal-content/EN/TXT/PDF/?uri=CELEX:31992L0043&from=EN > .

Council Directive 2009/147/EEC < http://eur-lex.europa.eu/LexUriServ/LexUriServ.do?uri=OJ:L:2010:020:0007:0025:EN:PDF > .

Crandall, R.M., Knight, T.M., 2018. Role of multiple invasion mechanisms and their interaction in regulating the population dynamics of an exotic tree. J. Appl. Ecol. 55, 885–894.

Da Luz, B.R., Crowley, J.K., 2010. Identification of plant species by using high spatial and spectral resolution thermal infrared (8.0–13.5 μm) imagery. Remote Sens. Environ. 114, 404–413.

De Sa', N.C., Carvalho, S., Castro, P., Marchante, E., Marchante, H., 2017. Using Landsat time series to understand how management and disturbances influence the expansion of an invasive tree. IEEE J. Sel. Top. Appl. Earth Obs. Remote Sens. 10 (7), 3243–3253.

Di Gregorio, A., Jansen, L.J.M., 2005. Land Cover Classification System (LCCS): classification concepts and user manual. Food and Agriculture Organization of the United Nations, Rome.

Dvorak, P., Mullerova, J., Bartalos, T., Bruna, J., 2015. Unmanned aerial vehicles for alien plant species detection and monitoring. In: The International Archives of the Photogrammetry, Remote Sensing and Spatial Information Sciences. XL-1/W4, 83-90.

ESA Sentinel, < https://sentinel.esa.int/web/sentinel/missions/sentinel-2 > .

Everitt, J.H., Yang, C., Deloach, C., 2005. Remote sensing of giant reed with quickbird satellite imagery. J. Aquatic Plant Manage. 43, 81–85.

Foody, G.M., Mathur, A., 2004. Toward intelligent training of supervised image classifications: directing training data for classification of complex forest areas. Remote Sens. Environ. 93, 107–117.

Foxcroft, L.C., Pyšek, P., Richardson D.M., Genovesi, P., 2013. Plant invasions in protected areas: patterns, problems and challenges. In: Foxcroft, L.C., Pysek, P., Richardson D.M., Genovesi, P. (Eds), Springer, pp 661. DOI: 10.1007/978-94-007-7750-7, ISBN 978-94-007-7749-1, ISBN 978-94-007-7750-7 (eBook).

Gavier-Pizarro, G.I., Kuemmerle, T., Hoyos, L.E., Stewart, S.I., Huebner, C.D., Keuler, N.S., Radeloff, V.C., 2012. Monitoring the invasion of an exotic tree (*Ligustrum lucidum)* from 1983 to 2006 with Landsat TM/ETM+ satellite data and Support Vector Machines in Cordoba, Argentina. Remote Sens. Environ. 122, 134–145.

Gavish, Y., O'Connel, J., Marsh, C.J., Tarantino, C., Blonda, P., Tomaselli, V., Kunin, W.E., 2018. Comparing the performance of flat and hierarchical habitat/land-cover classification models in a NATURA 2000 site. ISPRS J. Photogramm. Remote Sens. 136, 1–12.

Gitelson, A., Kaufman, Y., Merzlyak, M.N., 1996. Use of green channel in remote sensing of global vegetation from EOS-MODIS. Remote Sens. Environ. 58, 289–298.

Glenn, N.F., Mundt, J.T., Weber, K.T., Prather, T.S., Lass, L.W., Pettingill, J., 2005. Hyperspectral data processing for repeat detection of small infestations of leafy spurge. Remote Sens. Environ. 95 (3), 399–412.

Groβe-Stoltenbeg, A., Hellmann, C., Werner, C., Oldeland, J., Thiele, J., 2016. Evaluation of continuous VNIR-SWIR pectra versus narrowband hyperspectral indices to discriminate the invasive *Acacia longifolia* within a Mediterranean dune ecosystem. Remote Sens. 8, 334.

Groβe-Stoltenbeg, A., Hellmann, C., Thiele, J., Werner, C., Oldeland, J., 2018. Early detection of GPP-related regime shifts after plant invasion by integrating imaging spectroscopy with airborne LiDAR. Remote Sens. Environ. 209, 780–792.

Haralick, R.M., Sternberg, S.R., Zhuang, X., 1987. Image analysis using mathematical morphology. IEEE Transactions on Pattern Analysis and Machine Intelligence. PAMI-9 (4), 532–550.

Harris Geospatial Solution < https://www.harris.com/solution/envi > .

Horvath, G., 2003. Neural networks in system identification. In: Neural Networks for Instrumentation, Measurement and Related Industrial Applications, NATO Science Series. In: Ablameyko, S., Goras, L., Gori, M. and Piuri, V. (Eds.), IOS Press, Amsterdam, 185, 43–78.

Kowarik, I., 1995. Clonal growth in *Ailanthus altissima* on a natural site in West Virginia. J. Veg. Sci. 6, 853–856.

Kowarik, I., Saumel, I., 2007. Biological flora of Central Europe: A. altissima (Mill.) Swingle. Perspect. Plant Ecol. Evol. Syst. 8, 207–237.

LIFE12 BIO/IT/000213 < http://lifealtamurgia.eu/en/ > .

Lucas, R.M., Blonda, P., Bunting, P.F., Jones, G., Inglada, J., Arias, M., Kosmidou, V., Petrou, Z., Manakos, I., Adamo, M., Charnock, R., Tarantino, C., Mücher, S., Jongman, R., Kramer, H., Arvor, D., Honrado, J.P., Mairota, P., 2015. The Earth observation data for habitat monitoring (EODHaM) system. Int J Appl Earth Observ. Geoinform. 37, 17–28.

Ma, L., Li, M., Ma, X., Cheng, L., Du, P., Liu, Y., 2017. A review of supervised object-based land-cover image classification. ISPRS J. Photogramm. Remote Sens. 130, 277–293.

Mairota, P., Leronni, V., Xi, W., Mladenoff, D., Nagendra, H., 2013. Using spatial simulations of habitat modification for adaptive management of protected areas: Mediterranean grassland modification by woody plant encroachment. Environ. Conserv. 41, 144–146.

Mairota, P., Cafarelli, B., Labadessa, R., Lovergine, F., Tarantino, C., Lucas, R.M., Nagendra, H., Didham, R.K., 2015. Very high resolution Earth observation features for monitoring plant and animal community structure across multiple spatial scales in protected areas. Int. J. Appl. Earth Observ. Geoinform. 37, 100–105.

Mirik, M., Ansley, R.J., Steddom, K., Jones, D.C., Rush, C.M., Michels Jr, G.J., Elliott, N.C., 2013. Remote distinction of a noxious weed (musk thistle: *Carduus Nutans*) using airborne hyperspectral imagery and the support vector machine classifier.

Remote Sens. 5, 612–630.
Monteiro, A.T., Goncalves, J., Fernandes, R.F., Alves, S., Marcos, B., Lucas, R., Teodoro, A.C., Honrado, J.P., 2017. Estimating invasion success by non-native trees in a national park combining WorldView-2 very high resolution satellite data and species distribution models. Diversity 9, 1–18.
Mountrakis, G., Im, J., Ogole, C., 2011. Support vector machines in remote sensing: a review. ISPRS J. Photogramm. Remote Sens. 66, 247–259.
Müllerova, J., Bruna, J., Bartalos, T., Dvorak, P., Vitkovà, M., Pysek, P., 2017a. Timing is important: unmanned aircraft vs. satellite imagery in plant invasion monitoring. Front. Plant Sci. 8, 887.
Müllerova, J., Bartalos, T., Bruna, J., Dvorak, P., Vitkovà, M., 2017b. Unmanned aircraft in nature conservation: an example from plant invasions. Int. J. Remote Sens. 38 (8–10), 2177–2198.
Nagendra, H., Lucas, R.M., Honrado, J.P., Jongman, R., Tarantino, C., Adamo, P., Mairota, P., 2013. Remote sensing for conservation monitoring: assessing protected areas, habitat extent, habitat condition, species diversity and threats. Ecol. Ind. 33, 45–59.
Ng, W.T., Rima, P., Einzmann, K., Immitzer, M., Atzberger, C., Eckert, S., 2017. Assessing the potential of Sentinel-2 and Pleiades data for the detection of *Prosopis* and *Vachellia* spp. in Kenya. Remote Sens. 9, 1–74.
Niphadkar, M., Nagendra, H., Tarantino, C., Adamo, M., Blonda, P., 2017. Comparing pixel and object based approaches to map an understorey invasive shrub in tropical mixed forests. Front. Plant Sci. 8 (892), 1–18.
Olofsson, P., Foody, G.M., Stehman, S.V., Woodcock, C.E., 2013. Making better use of accuracy data in land change studies: estimating accuracy and area and quantifying uncertainty using stratified estimation. Remote Sens. Environ. 129, 122–131.
Olofsson, P., Foody, G.M., Herold, M., Stehman, S.V., Woodcock, C.E., Wulder, M.A., 2014. Good practices for estimating area and assessing accuracy of land change. Remote Sens. Environ. 148, 42–57.
Omer, G., Mutanga, O., Abdel-Rahman, E.M., Adam, E., 2015. Performance of support vector machines and artificial neural network for mapping endangered tree species using worldview-2 Data in Dukuduku Forest, South Africa. IEEE J. Sel. Top. Appl. Earth Obs. Remote Sens. 8, 4825–4840.
Peerbhay, K., Mutanga, O., Lottering, R., Ismail, R., 2016. Mapping *Solanum mauritianum* plant invasions using WorldView-2 imagery and unsupervised random forests. Remote Sens. Environ. 182, 39–48.
Pengra, B.W., Johnston, C.A., Loveland, T.R., 2007. Mapping an invasive plant, *Phragmites australis*, in coastal wetlands using the EO-1 Hyperion hyperspectral sensor. Remote Sens. Environ. 108 (1), 74–81.
Planchuelo, G., Catalán, P., Delgado, J.A., 2016. Gone with the wind and the stream: dispersal in the invasive species *Ailanthus altissima*. Acta Oecologica. 73, 31–37.
Pyšek, P., Richardson, D.M., 2010. Invasive species, environmental change and management, and health. Ann. Rev. Environ. Resour. 35, 25–55.
Qi, J., Chehbouni, A., Huete, A.R., Kerr, Y.H., 1994. Modified Soil Adjusted Vegetation Index (MSAVI). Remote Sens. Environ. 48, 119–126.
Regulation 1143/2014 < http://eur-lex.europa.eu/legal-content/EN/TXT/PDF/?uri=CELEX:32014R1143&from=EN > .
Richardson, D.M., Pysek, P., Rejmanek, M., 2000. Naturalization and invasion of alien plants: concepts and definitions. Divers. Distrib. 6, 93–107.
Sitzia, T., Campagnaro, T., Kowarik, I., Trentanovi, G., 2016. Using forest management to control invasive alien species: helping implement the new European regulation on invasive alien species. Biol. Invasions 18, 1–7.
Somers, B., Asner, G.P., 2013a. Invasive species mapping in Hawaiian rainforests using multi-temporal hyperion spaceborne imaging spectroscopy. IEEE J. Sel. Top. Appl. Earth Obs. Remote Sens. 6 (2), 351–359.
Somers, B., Asner, G.P., 2013b. Multi-temporal hyperspectral mixture analysis and feature selection for invasive species mapping in rainforests. Remote Sens. Environ. 136, 14–27.
Tarantino, C., Adamo, M., Pasquariello, G., Lovergine, F., Blonda, P., Tomaselli, V., 2012. 8-band image data processing of the worldview-2 satellite in a wide area of applications. Chapter in Earth Observation Book, Intech, ISBN 978-953-307-973-8, Ch. 6, doi: 10.5772/27499, pp. 137-152.
Tarantino, C., Adamo, M., Lucas, R., Blonda, P., 2016. Detection of changes in semi-natural grasslands by cross correlation analysis with WorldView-2 images and new Landsat 8 data. Remote Sens. Environ. 175, 65–72.
Tomaselli, V., Dimopoulos, P., Marangi, C., Kallimanis, A.S., Adamo, M., Tarantino, C., Panitsa, M., Terzi, M., Veronico, G., Lovergine, F., Nagendra, H., Lucas, R., Mairota, P., Mücher, S., Blonda, P., 2013. Translating land cover/land use classifications to habitat taxonomies for landscape monitoring: a Mediterranean assessment. Landscape Ecol. 28 (5), 905–930.
Trimble, 2014 < http://www.ecognition.com/suite > .
Turner, W., Rondinini, C., Pettorelli, N., Mora, B., Leidner, A.K., Szantoi, Z., Buchanana, G., Dech, S., Dwyer, J., Herold, M., Koh, L.P., Leimgruber, P., Taubenboeck, H., Wegmann, M., Wikelski, M., Woodcock, C., 2015. Free and open-access satellite data are key to biodiversity conservation. Biol. Conserv. 182, 173–176.
Ustin, S.L., DiPietro, D., Olmstead, K., Underwood, E., Scheer, G.J., 2002. Hyperspectral remote sensing for invasive species detection and mapping. IEEE Geosci. Remote Sens. Sympos. 3, 1658–1660.
Zheng, B., Myint, S.W., Thenkabail, P.S., Aggarwal, R.M., 2015. A support vector machine to identify irrigated crop types using time-series Landsat NDVI data. Int. J. Appl. Earth Observ. Geoinform. 34, 103–112.
Walker, G.A., Robertson, M.P., Gaertner, M., Gallien, L., Richardson, D.M., 2017. The potential range of Ailanthus altissima (tree of heaven) in South Africa: the roles of climate, land use and disturbance. Biol. Invasions 19, 3675–3690.
Wickert, K.L., O'Neal, E.S., Davis, D.D., Kasson, M.T., 2017. Seed production, viability, and reproductive limits of the invasive Ailanthus altissima (Tree-of-Heaven) within invaded environments. Forests 8, 226.